

## Optical gain at 1.54 $\mu\text{m}$ in erbium-doped silicon nanocluster sensitized waveguide

Hak-Seung Han, Se-Young Seo, and Jung H. Shin

Citation: *Appl. Phys. Lett.* **79**, 4568 (2001); doi: 10.1063/1.1419035

View online: <http://dx.doi.org/10.1063/1.1419035>

View Table of Contents: <http://apl.aip.org/resource/1/APPLAB/v79/i27>

Published by the [American Institute of Physics](#).

---

### Additional information on *Appl. Phys. Lett.*

Journal Homepage: <http://apl.aip.org/>

Journal Information: [http://apl.aip.org/about/about\\_the\\_journal](http://apl.aip.org/about/about_the_journal)

Top downloads: [http://apl.aip.org/features/most\\_downloaded](http://apl.aip.org/features/most_downloaded)

Information for Authors: <http://apl.aip.org/authors>

## ADVERTISEMENT



**Goodfellow**  
metals • ceramics • polymers • composites  
70,000 products  
450 different materials  
**small quantities fast**

[www.goodfellowusa.com](http://www.goodfellowusa.com)

## Optical gain at 1.54 $\mu\text{m}$ in erbium-doped silicon nanocluster sensitized waveguide

Hak-Seung Han, Se-Young Seo, and Jung H. Shin

*Department of Physics, Korea Advanced Institute of Science and Technology (KAIST), 373-1 Kusung-dong, Yuseong-gu, Taejeon, Korea*

(Received 30 May 2001; accepted for publication 10 September 2001)

Optical gain at 1.54  $\mu\text{m}$  in erbium-doped silicon-rich silicon oxide (SRSO) is demonstrated. Er-doped SRSO thin film was fabricated by electron-cyclotron resonance enhanced chemical vapor deposition of silicon suboxide with concurrent sputtering of erbium followed by a 5 min anneal at 1000 °C. Ridge-type single mode waveguides were fabricated by wet chemical etching. Optical gain of 4 dB/cm of an externally coupled signal at 1.54  $\mu\text{m}$  is observed when the Er is excited via carriers generated in the Si nanoclusters by the 477 nm line of an Ar laser incident on the top of the waveguide at a pump power of 1.5 W cm<sup>-2</sup>. © 2001 American Institute of Physics.

[DOI: 10.1063/1.1419035]

Silicon is the dominant semiconductor material, and has been called the “engine” behind the information revolution.<sup>1</sup> However, its poor optical activity due to its indirect band gap has led to its near exclusion from the field of optoelectronics whose exponential growth rate surpasses even the vaunted “Moore’s Law” of silicon integrated circuits.<sup>2</sup> This has motivated numerous attempts<sup>3</sup> at developing a silicon-based light source that would allow integrating information processing and optical communication capabilities into one single, silicon-based integrated structure. For such a structure to have a practical impact, however, more than just light emission is required. The light source should (1) emit light at a technologically important wavelength, (2) achieve its functionality under practical conditions (e.g., temperature and pump power), and (3) offer competitive advantage over existing technologies.

One material that has gathered much attention is Er-doped silicon. The light emission from Er-doped Si occurs due to the intra-4*f* shell atomic transition from the first excited state to ground state of Er<sup>3+</sup> (<sup>4</sup>I<sub>13/2</sub>→<sup>4</sup>I<sub>15/2</sub>). This transition emits light near 1.5  $\mu\text{m}$ , which is the standard wavelength for the optical telecommunication due to its coincidence with the absorption minimum of the silica-based optical fibers. Furthermore, theoretical<sup>4</sup> and experimental results<sup>5,6</sup> suggest that Er in Si is Auger-excited via carriers, generated either electrically or optically, that are trapped at Er-related defects and then recombine, and that this mechanism can be very efficient due to the strong carrier–Er interactions.

Unfortunately, the same strong carrier–Er interaction in Er-doped bulk Si can also severely reduce the efficiency of Er<sup>3+</sup> luminescence at practical temperature and pump powers down to impractical levels.<sup>5,6</sup> Recently, however, it has been demonstrated that by using silicon-rich silicon oxide (SRSO),<sup>7–9</sup> which consists of Si nanoclusters embedded in a SiO<sub>2</sub> matrix, many of the problems associated with bulk Si can be overcome such that efficient Er<sup>3+</sup> luminescence can be achieved.<sup>10,11</sup> In this case, Si nanoclusters act as classical sensitizer atoms that absorb incident photons and then transfer the energy to luminescent atoms (i.e., Er<sup>3+</sup>) except for the

following significant differences. First, the absorption cross section of Si nanoclusters is larger than that of Er<sup>3+</sup> ions by more than 3 orders of magnitude.<sup>12</sup> Second, as excitation occurs via Auger-type interaction between carriers in Si nanoclusters and Er<sup>3+</sup> ions, incident photons need not be resonant with one of the absorption bands of Er<sup>3+</sup>. Instead, they only need to create photocarriers in Si nanoclusters. In this letter, we demonstrate an optical gain at 1.54  $\mu\text{m}$  in an Er-doped SRSO waveguide. The Si nanoclusters excite Er, and also provide the refractive index contrast necessary for waveguiding. We observe gain in the optical signal at 1.54  $\mu\text{m}$  coupled into the waveguide when the waveguide is pumped from the top, and argue that such a waveguide satisfies all of the three aforementioned conditions necessary for a practical impact.

A 2.5  $\mu\text{m}$  thick Er-doped SiO<sub>x</sub> (*x*<2) film was deposited on a Si wafer with a 10  $\mu\text{m}$  thick thermal oxide by electron-cyclotron resonance plasma enhanced chemical vapor deposition with concurrent sputtering of Er using SiH<sub>4</sub> and O<sub>2</sub> as source gases. Details of the deposition process can be found in Ref. 9. The Si and Er content of the film was determined by Rutherford backscattering spectroscopy to be 34 and 0.03 at. %, respectively (not shown). After deposition, the film was rapidly thermal annealed at 1000 °C for 5 min both to activate Er and to precipitate Si nanoclusters. This particular composition and processing parameters were chosen to induce the optimum Er<sup>3+</sup> luminescence properties.<sup>13,14</sup> The photoluminescence (PL) spectrum of the annealed film was measured using the 477 nm line of an Ar laser, a grating monochromator, thermo-electrically cooled InGaAs or Si *p-i-n* diodes for the IR and visible region, respectively, and employing the standard lock-in technique. The 477 nm line was chosen because it does not coincide with any of the optical absorption bands of Er<sup>3+</sup>, thus ensuring that all Er<sup>3+</sup> are excited via Si nanoclusters and giving a good representation of a broad-band excitation source. The pump power used for photoluminescence (PL) was 200 mW. Ridge-type waveguides were fabricated by photolithography and wet chemical etching using buffered HF. After ridge formation, the waveguides were cut to a length of 9 mm, and had their

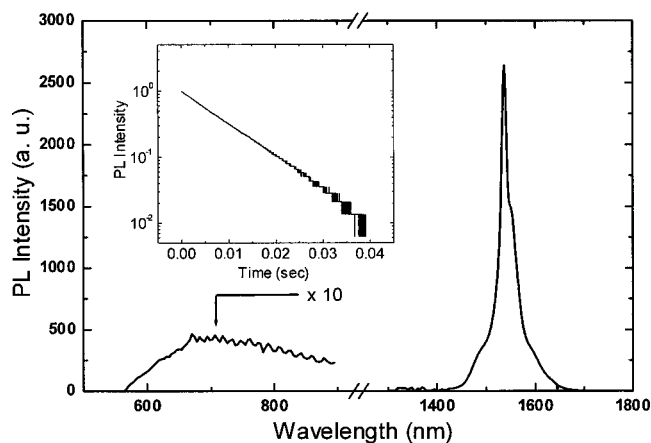


FIG. 1. The room temperature PL spectrum of the erbium-doped Si nanocluster film after annealing. The spectrum is corrected for the system response. Luminescence peaks typical of  $\text{Er}^{3+}$  near  $1.54 \mu\text{m}$  and that typical of Si nanoclusters near  $720 \text{ nm}$  are observed. The inset shows the decay trace of the  $\text{Er}^{3+}$  luminescence.

input and output facets polished mechanically. Optical gain was measured by coupling in an external  $1.537 \mu\text{m}$  signal from a DFB laser diode into the waveguide using a lensed fiber, and measuring the output coupled into the monochromator using a microscope objective. The input and output slits of the monochromator were opened to  $2.4 \text{ mm}$  in order to obtain the maximum signal, albeit at the cost of spectral broadening. The signal was modulated at  $11 \text{ Hz}$ , and detected using the standard lock-in technique. The input signal power was kept low ( $< 3 \mu\text{W}$ ). Again, the  $477 \text{ nm}$  line of the Ar laser was used as the pump beam. The pump beam was incident normal to the top surface of the waveguide. The pump beam size was  $1 \text{ cm} \times 0.1 \text{ cm}$ . The waveguide was pumped continuously, ensuring that only the external signal was detected via the lock-in amplifier. In all cases, measurements were performed at room temperature.

Figure 1 shows the PL spectrum of the film after the  $1000^\circ\text{C}$  anneal. The spectrum is corrected for the system response. We observe a PL peak at  $1.54 \mu\text{m}$  characteristic of  $\text{Er}^{3+}$  luminescence, and a broad peak centered near  $720 \text{ nm}$  that is characteristic of Si nanoclusters.<sup>15,16</sup> From the position of the Si nanocluster luminescence peak, we estimate the Si nanoclusters to be  $\sim 2 \text{ nm}$  in diameter,<sup>17</sup> corresponding to a nanocluster density of  $\sim 1 \times 10^{19} \text{ cm}^{-3}$ . Note that the luminescence due to Si nanoclusters is much weaker than that of  $\text{Er}^{3+}$ , indicating a high excitation efficiency of  $\text{Er}^{3+}$ . Furthermore, as the inset shows, the decay of the  $\text{Er}^{3+}$  luminescence upon termination of excitation is single exponential with a decay time of  $8.9 \text{ ms}$ , indicating a high luminescence efficiency of  $\text{Er}^{3+}$ .

Figure 2 shows the scanning electron microscope image of the fabricated ridge waveguide. The ridge is  $14 \mu\text{m}$  wide, and  $0.5 \mu\text{m}$  high. The inset [Fig. 2(a)] shows the ridge portion of the waveguide in detail. Note the smoothness of the surfaces due to the chemical nature of etching. Given the excess Si content of  $1 \text{ at. \%}$  and using the Maxwell-Garnett theory, we estimate the refractive index of the film to be  $1.464$  at  $1.54 \mu\text{m}$ , which is  $1.4\%$  larger than that of pure silica ( $1.444$  at  $1.54 \mu\text{m}$ ). Given these refractive indices, mode analysis using effective index method indicates that these waveguides are single mode. This is confirmed by the

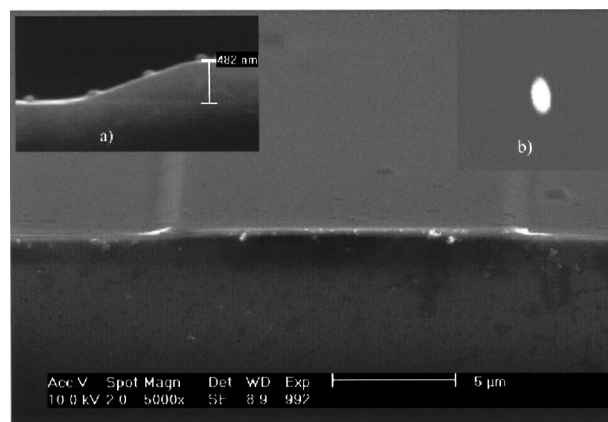


FIG. 2. Scanning electron microscope (SEM) image of a fabricated waveguide. Inset (a) shows the ridge in detail, and inset (b) shows the infrared CCD camera image of the transmitted beam, indicating that the waveguide is single mode.

inset [Fig. 2(b)], which shows an infrared charge-coupled device (CCD) camera image of the transmitted beam collected from the output facet using a microscope objective.

Figure 3 shows the spectra of the external signal input into the waveguide from a DFB laser diode at different pump powers. The inset shows the schematics of the experimental setup. We observe two peaks centered at  $1516$  and  $1537 \text{ nm}$  due to the laser diode. However, we do not observe any signal due to spontaneous  $\text{Er}^{3+}$  emission. This indicates that the lock-in method has filtered out all background signals, and confirms that any change we observe is due to the change in the intensity of the transmitted signal. We find that the signal intensity does not change significantly below a pump intensity of  $\sim 0.25 \text{ W cm}^{-2}$ . As the pump power is increased further, we observe a concomitant increase in the signal intensity, demonstrating optical gain of the external signal.

The gain spectra of the waveguide is shown in Fig. 4. The spectra are broadened because of the wide slit. However, a broad peak near  $1.54 \mu\text{m}$  typical of erbium can be clearly observed. The maximum amount of gain observed is  $4 \text{ dB/cm}$ , and it occurs at  $1.54 \mu\text{m}$ , in agreement with the peak of  $\text{Er}^{3+}$  luminescence spectrum shown in Fig. 1. Given the rela-

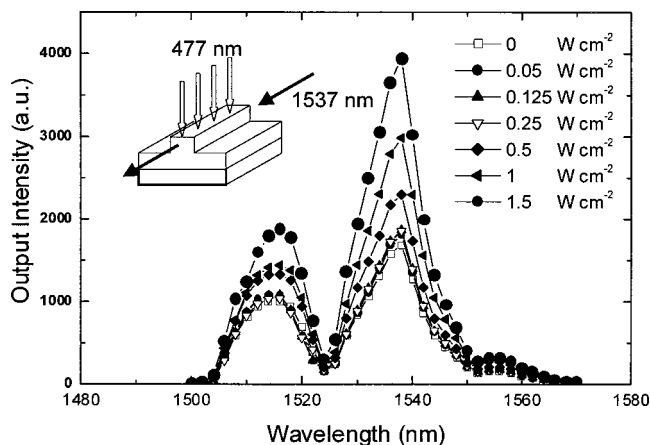


FIG. 3. The spectra of the external signal from a  $1537 \text{ nm}$  laser after being transmitted through the waveguide. The experimental setup used to measure the spectra is shown schematically in the inset. Note the increase in the transmitted signal as the pump power is increased beyond  $0.25 \text{ W cm}^{-2}$ .

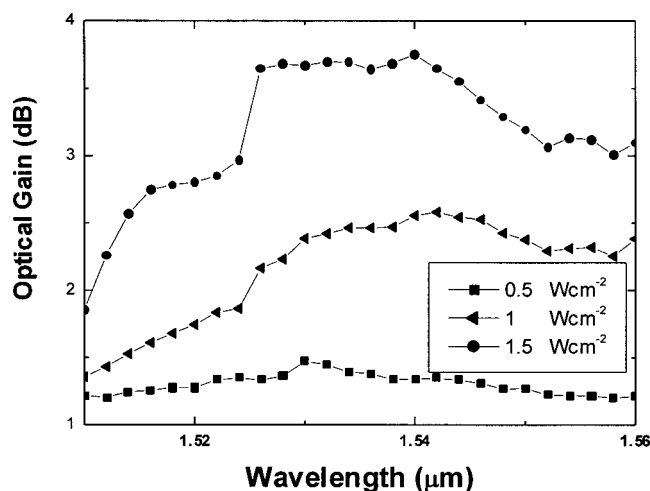


FIG. 4. The gain spectra obtained by dividing the spectra measured with the pump light on by the spectrum measured with the pump light off. The spectra are broadened because of the wide slit used. However, a clear peak at  $1.54 \mu\text{m}$  typical of  $\text{Er}^{3+}$  and in agreement with Fig. 1 can be observed.

tively low concentration of Er, the amount of gain is surprisingly large. We note, however, that because of the lack of a top cladding layer and the high refractive index contrast, the mode is strongly confined in the Er-doped SRSO layer. Furthermore, because of the geometry, Er ions in the entire illuminated region of  $1 \times 0.1 \text{ cm}$  are excited, resulting in a large overlap between the signal and the gain medium. Finally, the emission cross section of  $\text{Er}^{3+}$  in SRSO has been measured to be  $8 \times 10^{-20} \text{ cm}^2$ , which is much larger than that in homogenous  $\text{SiO}_2$  (typically of the order of  $1 \times 10^{-21} \text{ cm}^2$ ) presumably due to the strong asymmetry in the local dielectric environment of SRSO.<sup>18</sup> In fact, given the above values, the maximum gain possible in our waveguide is estimated to be 7 dB/cm.

Achieving such optical gain opens the possibility of developing a broad-band pumped, erbium-doped Si nanocluster amplifier. Such an amplifier would present several advantages. First, because its operating wavelength is near  $1.5 \mu\text{m}$ , it can be used immediately in the present optical communication network. Second, the requirements are very moderate. The power density of  $1.5 \text{ W cm}^{-2}$  is easily achievable with commercial blue-green light emitting diodes, and well within the tolerance of Si integrated circuits. The entire fabrication procedure is low cost and compatible with standard Si processing technology without any stringent demand for extreme measures. Note also that since Si nanoclusters only need to excite  $\text{Er}^{3+}$ , the need for control over their size distribution can be relaxed. Finally, because pumping can be achieved by a broad-band light source incident normally upon the amplifier, not only the pump laser and its control apparatus, but also the fiber and optical setup necessary to guide pump light into and out of the waveguide can be eliminated as well, significantly reducing the cost and difficulty of fabricating a waveguide amplifier. Note also that achieving

optical gain is the first step toward the realization of a Si-based laser. The significance of such a silicon-based laser operating in the  $1.5 \mu\text{m}$  wavelength region is that because Si is transparent in that wavelength region, it can be integrated with silicon-based modulators. As the switching speed of such modulators can be substantial (switches with nearly 10 Mhz switching speed have been demonstrated,<sup>19</sup> and Bragg-reflectors with 40 Ghz switching speed have been proposed),<sup>20</sup> such a structure may be a way to circumvent the problem of slow switching speed that has been pointed out to be a serious bottleneck in applying Si-based optoelectronics.<sup>21</sup>

In conclusion, we have demonstrated optical gain of 4 dB/cm at  $1.54 \mu\text{m}$  in erbium-doped Si nanoclusters at a pump density of  $1.5 \text{ W cm}^{-2}$ . This is an essential step toward realizing practical silicon-based optoelectronics, and offers the possibility of significantly impacting both Si technology and optical telecommunications.

The authors gratefully acknowledge S. Lee and D. H. Woo of Korea Institute of Science and Technology (KIST) for their support in fabricating the waveguides. This work was supported in part by Advanced Photonics Project and the University Research Program supported by Ministry of Information and Communications in South Korea.

<sup>1</sup> *Condensed Matter and Materials Physics* (National Research Council, National Academ Press, Washington, D. C., 1999).

<sup>2</sup> C. R. Giles, D. Bishop, and V. Aksyuk, *Mater. Res. Bull.* **26**, 328 (2001).

<sup>3</sup> See, for example, *Light emission from silicon: From Physics to Devices*, in *Semiconductors and Semimetals*, Vol. 49 (Academic, San Diego, 1998).

<sup>4</sup> I. N. Yassievich and L. C. Kimerling, *Semicond. Sci. Technol.* **8**, 718 (1993).

<sup>5</sup> J. Palm, F. Gan, B. Zheng, J. Michel, and L. C. Kimerling, *Phys. Rev. B* **54**, 17603 (1996).

<sup>6</sup> F. Priolo, G. Franzó, S. Coffa, and A. Carnera, *Phys. Rev. B* **57**, 4443 (1998).

<sup>7</sup> A. J. Kenyon, P. F. Trwoga, M. Federighi, and C. W. Pitt, *J. Phys.: Condens. Matter* **6**, L319 (1994).

<sup>8</sup> M. Fujii, M. Yoshida, Y. Kanazawa, S. Hayashi, and K. Yamamoto, *Appl. Phys. Lett.* **71**, 1198 (1997).

<sup>9</sup> J. H. Shin, M. Kim, S. Seo, and C. Lee, *Appl. Phys. Lett.* **72**, 1092 (1998).

<sup>10</sup> S. Seo and J. H. Shin, *Appl. Phys. Lett.* **75**, 4070 (1999).

<sup>11</sup> P. G. Kik, M. L. Brongersma, and A. Polman, *Appl. Phys. Lett.* **76**, 2325 (2000).

<sup>12</sup> G. Franzó, D. Pacifici, V. Vinciguerra, and F. Priolo, *Appl. Phys. Lett.* **76**, 2167 (2000).

<sup>13</sup> H.-S. Han, S.-Y. Seo, and J. H. Shin, *J. Appl. Phys.* **88**, 2160 (2000).

<sup>14</sup> S. Seo and J. H. Shin, *Appl. Phys. Lett.* **78**, 2709 (2001).

<sup>15</sup> K. S. Min, K. V. Shcheglov, C. M. Yang, Harry A. Atwater, M. L. Brongersma, and A. Polman, *Appl. Phys. Lett.* **69**, 2033 (1996).

<sup>16</sup> L. Pavesi, L. Dal Negro, C. Mazzoleni, G. Franzó, and F. Priolo, *Nature (London)* **408**, 440 (2000).

<sup>17</sup> D. J. Lockwood, *Solid State Commun.* **92**, 101 (1994).

<sup>18</sup> P. Kik, Ph.D. thesis, FOM-Institute for Atomic and Molecular Physics (AMOLF), Amsterdam, the Netherlands, 2000.

<sup>19</sup> C. Z. Zhao, A. H. Chen, E. K. Liu, and G. Z. Li, *IEEE Photonics Technol. Lett.* **9**, 1113 (1997).

<sup>20</sup> C. C. Wang, M. Currie, S. Alexandrou, and T. Y. Hsiang, *Opt. Lett.* **19**, 1453 (1994).

<sup>21</sup> P. Ball, *Nature (London)* **409**, 974 (2001).